Supporting Information:

Water flow enhancement in amorphous silica nanochannels coated with monolayer graphene

Enrique Wagemann,[†] Diego Becerra,[‡] Jens H. Walther,[¶,§] and Harvey A. Zambrano[*,‖]

†*Departamento de Ingeniería Mecánica, Facultad de Ingeniería, Universidad de Concepción, Concepción, Chile*

‡*Departamento de Ingeniería Química, Facultad de Ingeniería, Universidad de Concepción, Concepción, Chile*

¶*Department of Mechanical Engineering, Technical University of Denmark, Kgs Lyngby, Denmark*

§*Chair of Computational Science, ETH Zurich, Zurich, Switzerland*

‖*Department of Mechanical Engineering, Universidad Técnica Federico Santa María, Valparaiso, Chile*

E-mail: harvey.zambrano@usm.cl

Molecular Dynamics simulations overview

The atomistic simulations in this work were carried out using the parallel MD package FASTTUBE, which has been used extensively to study liquids confined inside CNTs, GE layers and silica channels.[S1] The water molecules are modeled using the rigid SPC/E water.[S2] The silica atoms are described using the TTAMm potential developed by Guissani and Guillot[S3] which is a modification of the classical TTAM potential developed by Tsuneyuki et al..[S4] In this study, we employ the original set of atomic partial charges in the TTAM model which correspond to values of: $q_{Si} = +2.4\,e$ and $q_{O_{SiO_2}} = -1.2\,e$. The van der Waals interactions between silica atoms and water molecules are described using a Buckingham potential with parameters taken from our previous work.[S5] The GE-water interactions are described by a Lennard-Jones potential parametrized by Werder et al.[S6] to reproduce a macroscopic water contact angle on graphite of 86°. The GE-silica interactions are described employing a Lennard-Jones potential with parameters from Zhang and Li[S7] which reproduce the proper substrate-regulated morphology of a supported GE layer. The carbon-carbon valence forces within the GE sheet are described using Morse, harmonic angle and torsion potentials.[S1] The leap-frog scheme is used to integrate the equations of motion with a time step of 2 fs. In all simulations, an orthorhombic box is used with periodic boundary conditions in the x and y directions, while free space conditions are applied in the z direction. The x and y dimensions are chosen to minimize artificial strain[S8] within the GE sheet due to the periodic boundary conditions. Temperature control is achieved by employing a Berendsen thermostat[S9] with a weak coupling constant of 0.1 ps. To this end, the position of the silicon and oxygen atoms within the outermost region of 0.4 nm width, measured from the external surface of each channel wall, is maintained fixed. Whereas silicon and oxygen atoms within the innermost region are maintained active and coupled to the Berendsen thermostat at 300 K. Note that in our NEMD simulations, the viscous Joule heat is removed by extracting heat through flexible solid walls therefore avoiding the effects on the flow of a thermostat connected directly to the fluid molecules. To account for the long range

electrostatic interactions, we employ a Smooth Particle Mesh Ewald (SPME) algorithm[S10] with a real-space cutoff of 1.0 nm that includes corrections for a slab geometry.[S11]

Interaction potentials and models

SPC/E Water model

The rigid extended Simple Point Charge SPC/E model[S2] is used to describe the water molecules in the system. This model corresponds to a rigid model of water, with an $O-H$ bond length of 0.1 nm and a $H-O-H$ angle of 109.47°. The bond lengths and intramolecular angle are fixed by employing the SHAKE algorithm.[S12] The intermolecular interactions consist of a Coulomb potential acting between partial charges on the oxygen ($q_O = -0.847e$) and hydrogen ($q_H = +0.4235e$) atoms and a Lennard-Jones potential acting between the oxygen atoms, that has the form:

$$U_{ij} = 4\epsilon_{\mathrm{OO}} \left[\left(\frac{\sigma_{\mathrm{OO}}}{r_{ij}} \right)^{12} - \left(\frac{\sigma_{\mathrm{OO}}}{r_{ij}} \right)^{6} \right] \tag{1}$$

with, $\sigma_{\mathrm{OO}} = 0.3166nm$ and $\epsilon_{\mathrm{OO}} = 0.650\ kJ/mol$.

Carbon-carbon interactions

The interactions between the carbon atoms within the graphene sheet are described using Morse, harmonic angle and torsional potentials.[S1] The bond and angle torsion terms are original obtained from reference[S13] and successfully reproduce the structures of graphite and fullerene crystals. The torsion term is employed to maintain the structural properties in graphene sheets.[S1] The potential has the form:

$$U(r_{ij}, \theta_{ijk}, \phi_{ijkl}) = K_{Cr}(\xi_{ij} - 1)^2 + \frac{1}{2} K_{C\theta}(cos\theta_{ijk} - cos\theta_C)^2 + \frac{1}{2} K_{C\phi}(1 - cos2\phi_{ijkl}) \tag{2}$$

where: θ_{ijk} represents the bending angle, ϕ_{ijkl} is the torsion angle, r_{ij} is the distance between atoms (nm), $\xi_{ij} = e^{-\gamma(r_{ij}-r_c)}$, $K_{Cr} = 47890\ \frac{kJ}{Molnm^2}$, $K_{C\phi} = 562.2\ \frac{kJ}{mol}$, $r_C = 0.1418\ nm$, $\theta_C = 120.0°$ and $\gamma = 21.867\ nm^{-1}$

The non bonding interactions in graphene are described using Lennard-Jones potentials, whose parameters are obtained from the Universal Force Field. [S14]

Silica-silica interactions

The interactions between silica atoms are described using the TTAMm potential. [S3] The TTAMm is a modification of the classical TTAM model developed by Tsuneyuki et al. [S4] The partial charges for this potential are: $q_{Si} = +2.4e$ and $q_O = -1.2e$. The potential has the following form:

$$U_{ij} = \frac{q_i q_j}{4\pi\epsilon_0 r_{ij}^2} + \alpha_{ij} exp\left(-r_i j \rho_{ij}\right) - \frac{C_{ij}}{r_{ij}^6} + 4\epsilon_{ij}\left[\left(\frac{\sigma_{ij}}{r_{ij}}\right)^{18} - \left(\frac{\sigma_{ij}}{r_{ij}}\right)^{6}\right] \tag{3}$$

with the following parameters:

Table S1: Silica interaction parameters

Pair	$\epsilon_{ij}\ (kJ/mol)$	$\sigma_{ij}\ (nm)$	$C_{ij}\ (kJ\,nm^6/mol)$	$\alpha_{ij}\ (kJ/mol)$	$\rho_{ij}\ (nm^{-1})$
Si-Si	$1.277 \cdot 10^3$	0.040	$2.240 \cdot 10^{-3}$	$8.417 \cdot 10^{10}$	$1.522 \cdot 10^2$
Si-O	1.083	0.130	$6.82510 \cdot 10^{-3}$	$1.0347 \cdot 10^6$	$0.480 \cdot 10^2$
O-O	$4.60 \cdot 10^{-2}$	0.220	$2.07 \cdot 10^{-2}$	$1.696 \cdot 10^5$	$0.283 \cdot 10^2$

Water-carbon interactions

The water-carbon interactions are described using the potential calibrated by Werder et al. [S6] which reproduces a macroscopic WCA of 86°. This potential corresponds to a pairwise additive Lennard-Jones potential between the oxygen of the water and the carbon atoms, with $\sigma = 0.319\ nm$ and $\epsilon = 0.392\ kJ/mol$

Water-silica interactions

The van der Waals interactions between silica atoms and water molecules are described using a Buckingham potential calibrated by Zambrano et al. [S5] to reproduce the experimental WCA of 19.9° measured by Thamdrup et al.[S15] The parameters of the potential are listed in the following table:

Table S2: Water-silica interaction parameters

Pair	C_{ij} $(kJ\,nm^6/mol)$	α_{ij} (kJ/mol)	ρ_{ij} (nm^{-1})
O_{SiO_2}-H_{H_2O}	0.0	6830.682	32.65839
Si-O_{H_2O}	0.0240	101298.0707544	25.0

Carbon-silica interactions

The carbon-silica interactions are described employing a Lennard Jones potential with parameters from Zhang and Li [S7] which reproduces the proper substrate-regulated morphology of a supported GE layer. The parameters for this potential are summarized in the following table:

Table S3: Graphene-silica interaction parameters

Pair	ϵ_{ij} (kJ/mol)	σ_{ij} (nm)
C-Si	0.20551	0.1506
C-O_{SiO_2}	0.48145	0.2256

Substrate details

Silica slab amorphization

The silica slabs are created by replicating a β crystoballite unit cell and then applying a thermal annealing to the crystalline silica.

Coated silica substrates

The amorphous silica substrate coated by a graphene layer is obtained by using the following protocols; First, a cristobalite unit cell is replicated to build a crystalline slab. Then, the slab amorphization is achieved by following the annealing procedure reported by Zambrano et al.[S5] The initial slab dimensions are; 4.424 nm × 10.744 nm × 2.528 nm. Each slab is composed of 3808 Si atoms and 7616 O atoms. The simulation box dimensions are 4.666476 nm × 11.0604 nm × 15 nm (periodic boundary condition are applied along the x and y direction, while free space condition is given along the z direction). The atoms within each slab interact with each other, but not with the atoms of the other slab. A timestep of 1 fs is used. The Si and O atoms are connected to a Berendsen thermostat, with a coupling constant of 0.005 ps. The silica is first heated to 3000 K for 10 ps, then the system is quenched to 300 K using a cooling rate of 70 K/ps. After the target temperature is reached the system is given more time to equilibrate (the total simulation time is 100 ps). Subsequently, the substrate is coated by releasing a GE sheet near the silica surface. Afterward, the system is equilibrated by connecting the carbon atoms to a Berendsen thermostat at 300 K while silica atoms are maintained fixed. After the equilibrium state is reached, we characterize the coated substrate. Measured C-C bond mean distance correspond to 0.1423 nm, representing a stretch of 0.34%.

We find that the silica surface present a standard deviation of the distribution of heights of 0.38 nm, while the GE coating presents a standard deviation of the distribution of heights of 0.1 nm. These results imply that the use of graphene as a coating can reduce the surface roughness of the substrate to approximately 40% its original value. Moreover, a GE-silica contact separation of 0.40 nm is computed, in agreement to the experimental value reported by Ishigami et. al..[S16] Furthermore, an average C-C bond length of 0.1423 nm is computed, demonstrating low strain in the GE layer.

Solvent Accessible Surface Area

Solvent Accessible Surface Area (SASA) was calculated for each surface using the SASA command provided in VMD.[S17] An expanded atom radius of 2 Å was used for this purpose. The SASA was calculated for the atoms with position within 0.3 nm and 43 nm along the x axis and within positions between 0.3 nm and 10.0 nm, along the y axis. This section of the slab has a projected area in the xy plane of 38.80 nm^2. As a reference the SASA of a flat pristine graphene sheet was also measured. The following SASAs were obtained; 4159 $Å^2$ for the pristine graphene, 42.88 nm^2 for the graphene on top of a silica slab and 55.21 nm^2 for the silica surface. The resulting SASA per projected area for each case is 1.072 for the pristine graphene sheet, 1.105 for the graphene layer on top of the silica surface and 1.422 for the silica surface.

Contact distance

Contact distance is estimated by measuring the distance between the atoms in the GE layer and the surface atoms of the underlying silica. This distance was computed by averaging the minimum distance between each carbon atom in the GE and the atoms of the silica substrate.

Height standard deviation

The standard deviation of the height of the silica surface is measured by employing a binning sampling method. The bins have a size of 0.2 nm in the x and $y-$direction. In each bin, the height was computed by comparing the height of all the atoms inside the bin, and the maximum height which is defined as the height of the bin (for the upper slab it was defined as the minimum height). Then, the computed heights are averaged and the standard deviation is calculated.

Water contact angle measurement

In order to validate the atomistic models and the force fields employed in our simulations, the WCA is measured on both GE coated and bare silica substrates. To this end, MD simulations of periodic cylindrical droplets of water are conducted to reproduce directly the macroscopic WCA, avoiding the line tension effects associated to spherical droplets.[S18] A snapshot of the system employed for the coated substrate case is presented in Figure S1 A. First, we equilibrate a periodic water droplet consisting of 3600 water molecules in the NVT ensemble at 300 K during 0.5 ns. After equilibrium state is reached, the droplet is released 0.5 nm away from the substrate surface. The water molecules are connected to the thermostat during the first 0.5 ns of simulation, then the system is equilibtrated for another 0.5 ns in the NVE ensemble. Trajectory data are collected every 0.1 ps during 1 ns of simulation. The density profiles are computed by a binning sampling method. The WCA is evaluated by fitting a circle to the 650 kg/m^3 isochore,[S19] as shown on Figure S1 B. The near wall region is excluded from the fit to avoid the influence from density fluctuations at the liquid-solid interface. For more details about the methodology to measure the WCA, the reader is referred to the supporting material.

The WCA measured for the droplet on the silica substrate coated with the GE sheet is 49°, in agreement with the WCA reported by Rafiee et al.[S18] Furthermore, complete wetting is achieved for water on the bare silica substrate. Moreover, we notice that when comparing the measured WCA for the cases with coated and uncoated silica, the observed wettability values are in line with the GE translucency to wettability reported by Shih et al.[S20] and Rafiee et al.[S18] wherein the WCAs were measured on GE layers supported on fused silica substrates.

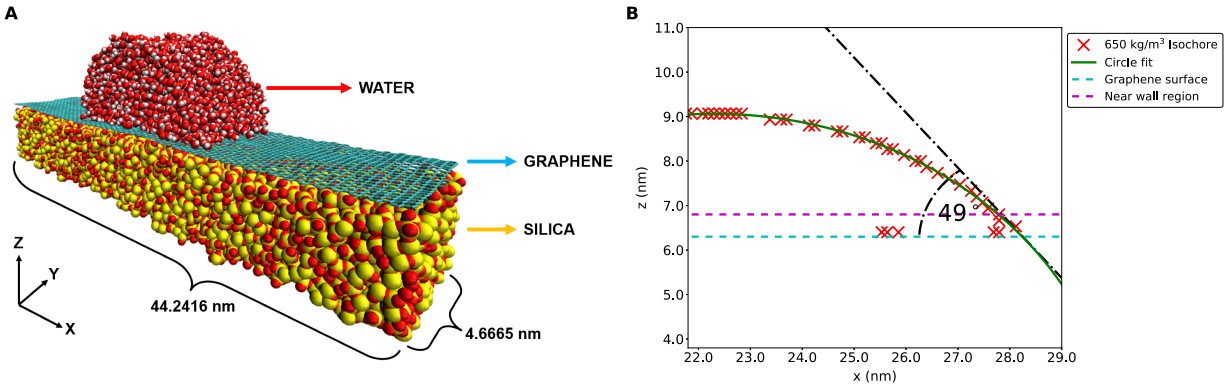

Figure S1: A) Snapshot of a simulation of the water contact angle. A nanodroplet is simulated on a GE coated silica substrate, the cylindrical shape of the droplet avoid the effect of the line tension on the measured angle. B) Water contact angle is measured by a circular fitting to the droplet interface.

Channel filling

An internal pressure of 1 bar is achieved by using the bottom slab as a piston, while the top one is kept fixed. To this end an acceleration of 0.000135888 nm/ps^2 in the positive z direction is imposed to all the Si and O atoms of the bottom slab. The water molecules are coupled to the thermostat to attain a temperature of 300 K during the entire simulation. After steady state is reached, which is ensured by verifying the center of mass position of the botom silica slab is not changing, the atoms in the outermost region of 0.4 nm width, measured from the external surface of each slab, are maintained fixed. The rest of the silica atoms (in both slabs) are maintain active and coupled to the thermostat at 300 K. The number of water molecules within each studied channel are: 3437 for the channel with height of 2.4nm, 5156 for the channel with height of 3.4 nm and 6800 for the channel with height of 4.4 nm. The water confined in the channel is equilibrated for 2 ns and density profiles are extracted using a binning sampling method.

Temperature profile

The temperature profile for the case with channel height of 3.4 nm and an applied external field of $9.324 \cdot 10^{11} m/s^2$ is presented in Figure S2.

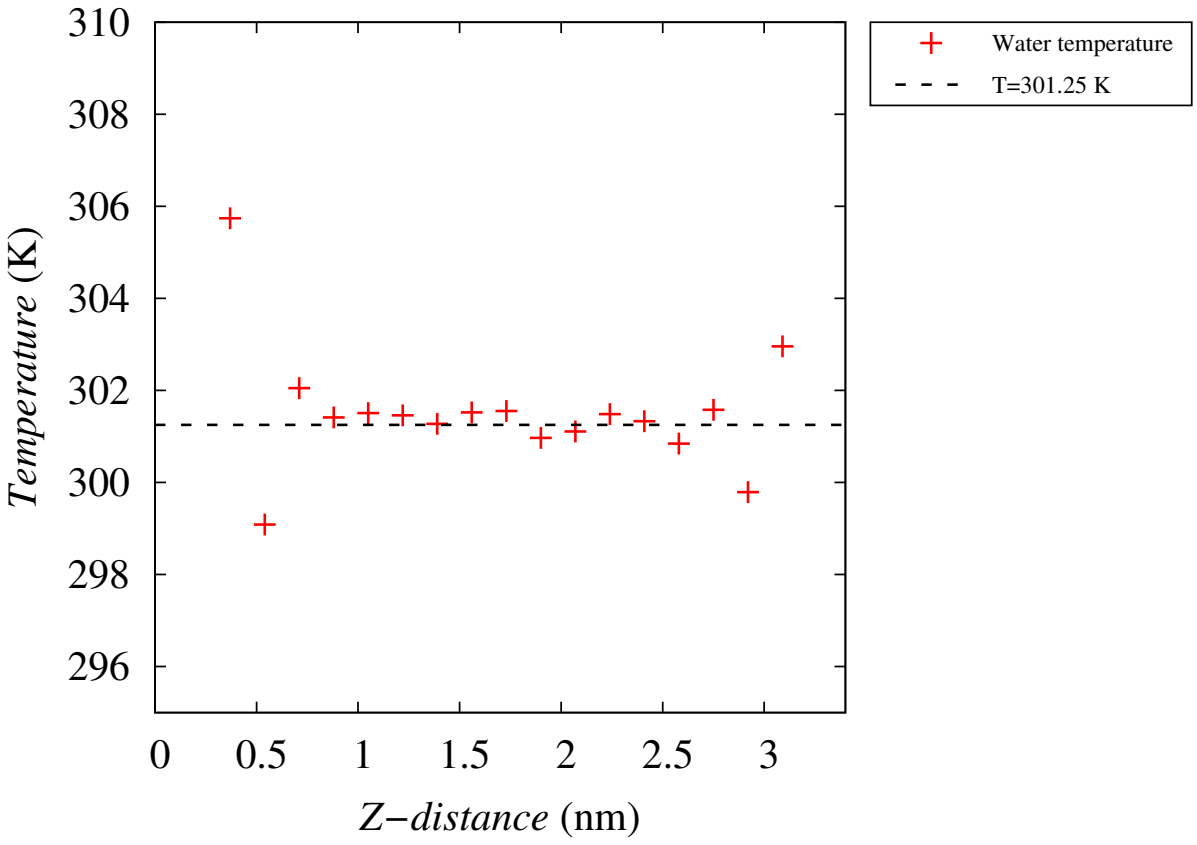

Figure S2: Temperature profile for the case with 3.4 nm channel height with an applied external field of $9.324 \cdot 10^{11} m/s^2$.

Binning sampling method

The used binning sampling method divides the simulation box in the z dimension (for the velocity and density profile calculation) in bins of $0.113333\,nm$ height. Velocity profiles are computed by dividing the sum of momemtum of all the particles over time, per bin, by the sum of the total mass in each bin. This can be summarized by the formula:

$$u_k = \frac{\sum_i^{n_k} m_i v_i}{\sum_i^{n_k} m_i}$$

density profiles are computed by dividing the sum of all mass per bin over time by the number of time steps averaged and the bin's volume;

$$\rho_k = \frac{\sum_i^{n_k} m_i}{N \cdot V_k}$$

In the WCA cases the box is divided along the x and z direction in bins with size of $0.113333\,nm$.

Volumetric flow calculation

Volumetric flow is calculated from the mass flow. The mass flow was measured by computing and averaging the number of molecules crossing 20 equidistant fixed planes in the streaming direction per unit of time. The mass flow is then divided by the overall density of the fluid in the channel to obtain the volumetric flow.

Computed hydrodynamic properties for water confined in coated and uncoated channels

Table S4 lists the computed hydrodynamic properties for water confined in the studied channels.

Table S4: Calculated hydrodynamic properties for the water flow inside the coated silica channels. h denotes the channel height, ϵ the flow enhancement, l_s the slip length, μ_{eff} the effective viscosity, h^* the bare channel height and ϵ^* the "effective" flow enhancement

h (nm)	ϵ	l_s (nm)	μ_{eff} (mPa·s)	h^* (nm)	ϵ^*
2.4	11.3 ± 0.5	3.09 ± 0.26	0.654 ± 0.05	3.0	3.72 ± 0.15
3.4	7.8 ± 0.2	2.99 ± 0.32	0.662 ± 0.08	4.0	3.49 ± 0.07
4.4	6.0 ± 0.1	2.93 ± 0.09	0.658 ± 0.02	5.0	3.21 ± 0.07

Effective enhancement as a function of channel height

The "effective" enhancement as a function of the channel height is presented in figure S3. The "effective" enhancement is calculated as the ratio between the volumetric flow rate measured within a GE coated silica channel and the volumetric flow rate measured within the corresponding uncoated channel. The available channel height for the coated channel is estimated as the distance between graphene layers, subtracting the van der Waals size of the carbon atoms (0.34 nm). The available channel height for the uncoated cases is estimated as the distance between graphene layers in the coated channels, adding 0.6 nm.

Orientation function

The behavior of interfacial polar liquids like water depends strongly on the properties of the confining surface, in particular, water molecular orientation and surface wetting are strongly related.. To gain further insight into the graphene coating effect on the hydrodynamic properties of interfacial water within the channel, the average orientation of the water dipole vector is computed. The orientation function is described by:

$$f(z_i) = \left\langle \sum_{i=1}^{n(z_i)} \frac{\cos \alpha}{n(z_i)} \right\rangle \tag{4}$$

where z_i is the distance along z axis measured from the silica surface for the pristine channel or from the equimolar dividing surface with water density of $650 kg/m^3$ for the GE coated channel, α is the angle between the water dipole vector and the normal vector to the

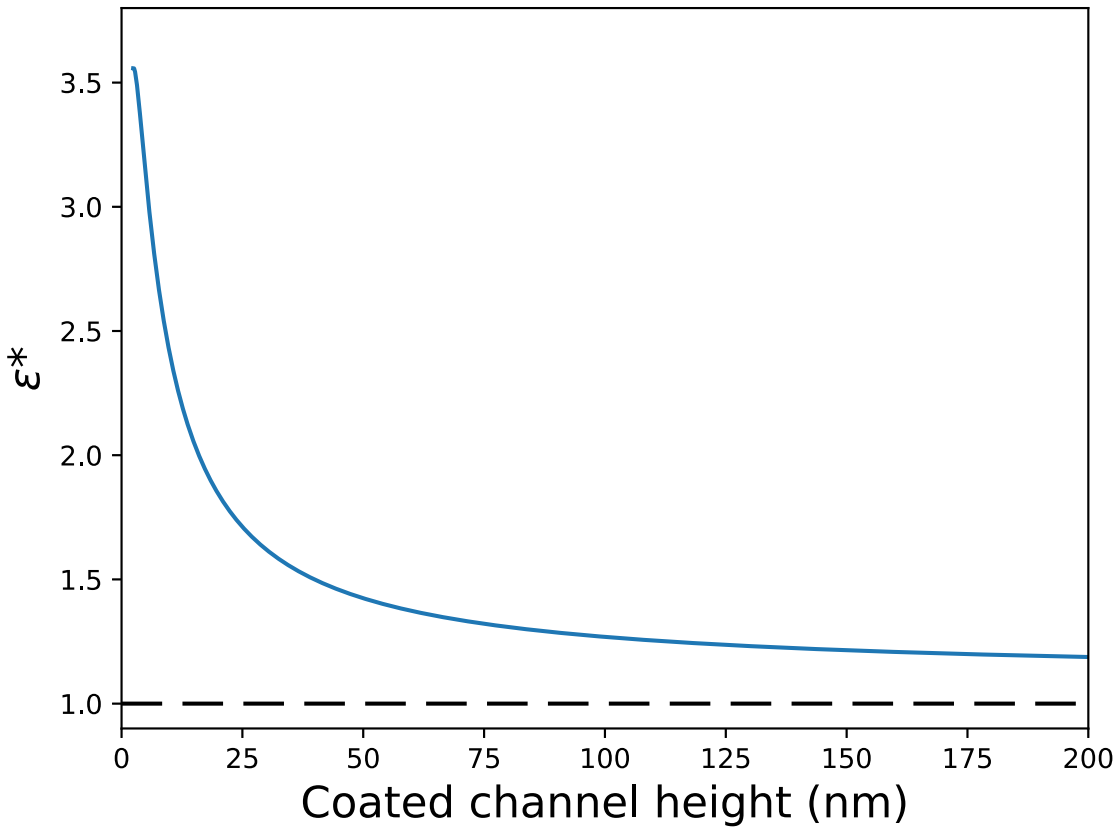

Figure S3: Effective enhancement as a function of coated channel height. Effective enhancement decreases with increase in the channel height, asymptotically reaching the unity at large heights.

solid surface (Figure S4), $n(z_i)$ is the number of water molecules within z_i and $z_i + \Delta z$, Δz is the bin size along z axis and set to 0.8 Å, and $\langle \cdots \rangle$ represents time average.

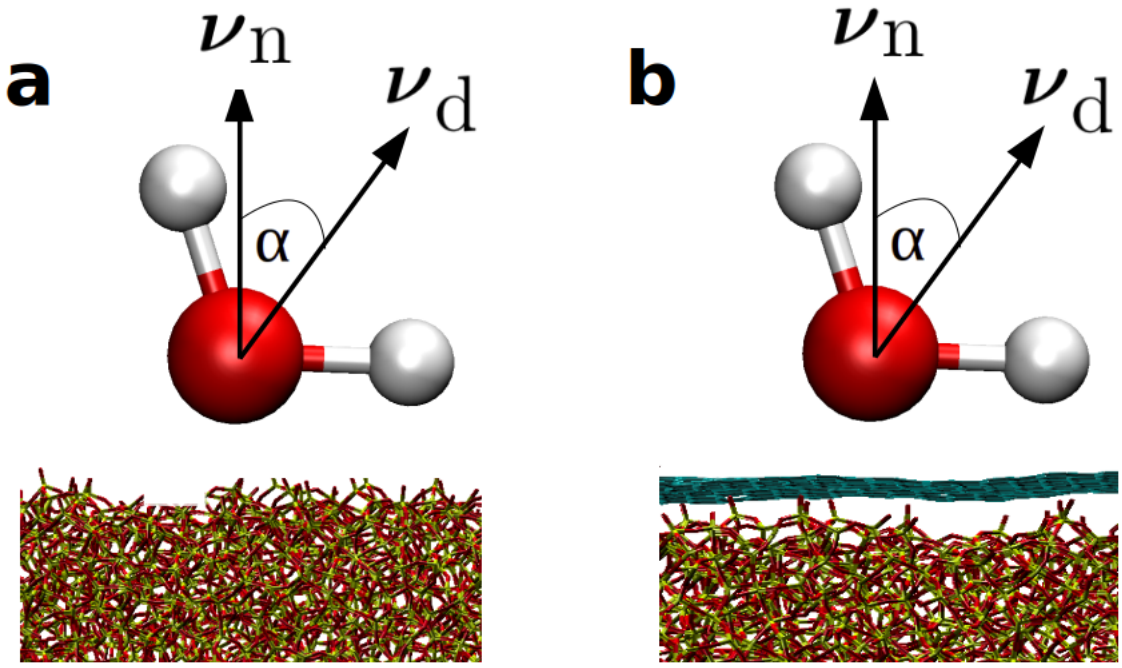

Figure S4: Sketch of the angle α set as the angle between the water dipole vector ($\boldsymbol{\nu}_d$) and the normal vector to a) the pristine silica surface or b) the silica surface with graphene coating ($\boldsymbol{\nu}_n$).

References

References

(S1) Walther, J. H.; Jaffe, R.; Halicioglu, T.; Koumoutsakos, P. Carbon nanotubes in water: Structural characteristics and energetics. *J. Phys. Chem. B* **2001**, *105*, 9980–9987.

(S2) Berendsen, H. J. C.; Grigera, J. R.; Straatsma, T. P. The missing term in effective pair potentials. *J. Phys. Chem.* **1987**, *91*, 6269–6271.

(S3) Guissani, Y.; Guillot, B. A numerical investigation of the liquid-vapor coexistence Curve of Silica. *J. Chem. Phys.* **1996**, *104*, 7633–7644.

(S4) Tsuneyuki, S.; Tsukada, M.; Aoki, H.; Matsui, Y. First-principles interatomic potential of silica applied to molecular dynamics. *Phys. Rev. Lett.* **1988**, *61*, 869–874.

(S5) Zambrano, H.; Walther, J. H.; Jaffe, R. Molecular dynamics simulations of water on a hydrophilic silica surface at high air pressures. *J. Mol. Liq.* **2014**, *198*, 107–113.

(S6) Werder, T.; Walther, J. H.; Jaffe, R. L.; Halicioglu, T.; Koumoutsakos, P. On the water-graphite interaction for Use in MD simulations of graphite and carbon nanotubes. *J. Phys. Chem. B* **2003**, *107*, 1345–1352.

(S7) Zhang, Z.; Li, T. A molecular mechanics study of morphologic interaction between graphene and Si nanowires on a SiO 2 substrate. *Journal of Nanomat.* **2011**, *2011*, 1–7.

(S8) Xiong, W.; Liu, J. Z.; Ma, M.; Xu, Z.; Sheridan, J.; Zheng, Q. Strain engineering water transport in graphene nanochannels. *Phys. Rev. E* **2011**, *84*, 056329.

(S9) Berendsen, H. J. C.; Postma, J. P. M.; van Gunsteren, W. F.; DiNola, A.; Haak, J. R. Molecular dynamics with coupling to an external bath. *J. Chem. Phys.* **1984**, *81*, 3684–3684.

(S10) Essmann, U.; Perera, L.; Berkowitz, M. L.; Darden, T.; Lee, H.; Pedersen, L. G. A smooth particle mesh Ewald method. *J. Chem. Phys.* **1995**, *103*, 8577–8593.

(S11) Yeh, I.-C.; Berkowitz, M. L. Ewald summation for systems with slab geometry. *J. Chem. Phys.* **1999**, *111*, 3155–3162.

(S12) Ryckaert, J.-P.; Ciccotti, G.; Berendsen, H. J. Numerical integration of the cartesian equations of motion of a system with constraints: molecular dynamics of n-alkanes. *J. Comput. Phys.* **1977**, *23*, 327–341.

(S13) Quo, Y.; Karasawa, N.; Goddard III, W. A. Prediction of fullerene packing in C60 and C70 crystals. *Nature* **1991**, *351*, 464.

(S14) Rappé, A. K.; Casewit, C. J.; Colwell, K.; Goddard Iii, W.; Skiff, W. UFF, a full periodic table force field for molecular mechanics and molecular dynamics simulations. *J. Am. Chem. Soc.* **1992**, *114*, 10024–10035.

(S15) Thamdrup, L. H.; Persson, K. F.; Bruus, H.; Kristensen, A.; Flyvbjerg, H. Experimental investigation of bubble formation during capillary filling of SiO2 nanoslits. *Appl. Phys. Lett.* **2007**, *91*, 1–3.

(S16) Ishigami, M.; Chen, J.; Cullen, W.; Fuhrer, M.; Williams, E. Atomic structure of graphene on SiO2. *Nano Lett.* **2007**, *7*, 1643–1648.

(S17) Humphrey, W.; Dalke, A.; Schulten, K. VMD: visual molecular dynamics. *J. Mol. Graph.* **1996**, *14*, 33–38.

(S18) Rafiee, J.; Mi, X.; Gullapalli, H.; Thomas, A. V.; Yavari, F.; Shi, Y.; Ajayan, P. M.; Koratkar, N. A. Wetting transparency of graphene. *Nature Mat.* **2012**, *11*, 217–222.

(S19) Werder, T.; Walther, J. H.; Jaffe, R. L.; Halicioglu, T.; Noca, F.; Koumoutsakos, P. Molecular dynamics simulation of contact angles of water droplets in carbon nanotubes. *Nano Lett.* **2001**, *1*, 697–702.

(S20) Shih, C.-J.; Wang, Q. H.; Lin, S.; Park, K.-C.; Jin, Z.; Strano, M. S.; Blankschtein, D. Breakdown in the wetting transparency of graphene. *Phys. Rev. Lett.* **2012**, *109*, 176101.